공학석사 학위논문

Impedance-Based Biosensor for Extracellular Vesicles Detection Using Surface Modified Gold Nanoparticles

표면 개질 된 금나노입자를 활용한 임피던스 기반 세포외소포 검출 바이오센서

2020 년 8 월

서울대학교 대학원

융합과학부 나노융합전공

정 한 나

Impedance-Based Biosensor for Extracellular Vesicles Detection Using Surface Modified Gold Nanoparticles

표면 개질 된 금나노입자를 활용한 임피던스 기반 세포외소포 검출 바이오센서

지도 교수 이 강 원
이 논문을 공학석사 학위논문으로 제출함
2020 년 7 월

서울대학교 대학원
융합과학부 나노융합전공
정 한 나

정 한 나의 공학석사 학위논문을 인준함
2020 년 7 월

위 원 장 김 연 상 (인)

부위원장 이 강 원 (인)

위 원 송 윤 규 (인)

Abstract

Impedance-Based Biosensor for Extracellular Vesicles Detection Using Surface Modified Gold Nanoparticles

Han Na Jung

Program in Nano Science and Technology

Graduate School of Convergence Science and Technology

Seoul National University

Exosome is an extracellular vesicles (EVs) that have become a rising interest for the past decade due to its important role in intercellular communications as well as containing biological molecules such as genetic materials and proteins that can be used as diagnostic tools to detect various diseases. However, the challenge is

found in detecting and analyzing the nano-sized extracellular vesicles. Other conventional known methods to detect and analyze EVs require complex experimental procedures, and it is time-consuming. In this study, we present an interdigitated electrode (IDE) impedance-based biosensor that detects the captured EVs through impedance measurement. The impedance of the captured EVs was 1.06 kΩ and has increased to 16.14 kΩ after EVs were captured onto the fabricated biosensor. The impedance further increased to 19.33 kΩ as anti-CD63 conjugated gold nanoparticles were bound onto the captured EVs. This shows that the additional binding of the gold nanoparticle has enhanced the sensitivity of the impedance. Therefore, the proposed impedance-based biosensor with the application of surface modified gold nanoparticles shows a promising platform that is capable to detect extracellular vesicles as a diagnostic tool in clinical application.

Keywords: Extracellular Vesicles, Exosome, Impedance-Based, Biosensor, Gold Nanoparticles

Student Number: 2018-27795

Table of Content

List of Tables

List of Figures

Chapter 1. Introduction.

Exosomes are small extracellular vesicles with a size of 30–150nm that have increased in their interest over the past decade [1]. Exosomes are released from all eukaryotic cells. They were recently found to play an important role in intercellular communication and carry various active biological molecules such as proteins, lipids, nucleic acids, mRNAs, and microRNAs shown in Figure 1. Because of the specific biological molecules that exosomes contain, it enables researchers to track down the origin cell of where the exosomes were released. This unique characteristic property of exosome suggests the potential of using exosome as a biomarker to diagnose various diseases such as cardiovascular diseases, neurodegenerative diseases, different types of tumors, and other more [2–5]. However, isolating and efficiently measuring the detection of small size and low dense of exosomes remain a challenge. The current known conventional methods of detecting and analyzing exosomes are time–consuming and require complex experimental procedures [6, 7]. Regardless of its challenges, various diagnostic tools [5, 8–13] and methods are being researched, such as optically [14–16], electrically [17, 18], and mechanically [19–21] to detect

biomaterials like exosomes.

Electrochemical impedance spectroscopy (EIS) is one of the electrical methods that is a widely integrated analytical tool to detect and quantify targeting molecules of interest. Unlike other methods such as potentiometry and amperometry, EIS does not necessarily need a redox probe, which makes this method a fast and simple detecting method as well as less complex in the sensor fabrication process. Therefore, EIS makes it a suitable and promising technique to apply in the biomedical point-of-care test [22-24]. The impedance is an input of a small sinusoidal voltage, in which the resulting current is computed as a function of frequency [25, 26]. Therefore, by the electrode surface alternation and through the binding of biomolecules, a measurable interfacial impedance changes as it is induced [24, 27]. The sensitivity of the sensor is determined by the electrode gap width and the electric field strength that is generated between the electrodes [28]. The integration of the gold nanoparticles (AuNPs) can also improve the sensitivity of the EIS sensor [29].

In this research, an EIS biosensor was fabricated for the selective and label-free detection of exosomes derived from plasma. In addition, binding of the anti-CD63, an exosome marker protein, conjugated AuNPs took place to enhance the detecting sensitivity of

the exosomes. The selectively captured exosomes and the binding of the anti-CD63 conjugated AuNPs were then analyzed through impedance measurement to observe the change in its impedance. Figure 2 shows an illustration of the overall scheme of the interdigitated electrode (IDE) impedance-based biosensor with sensor fabrication layer.

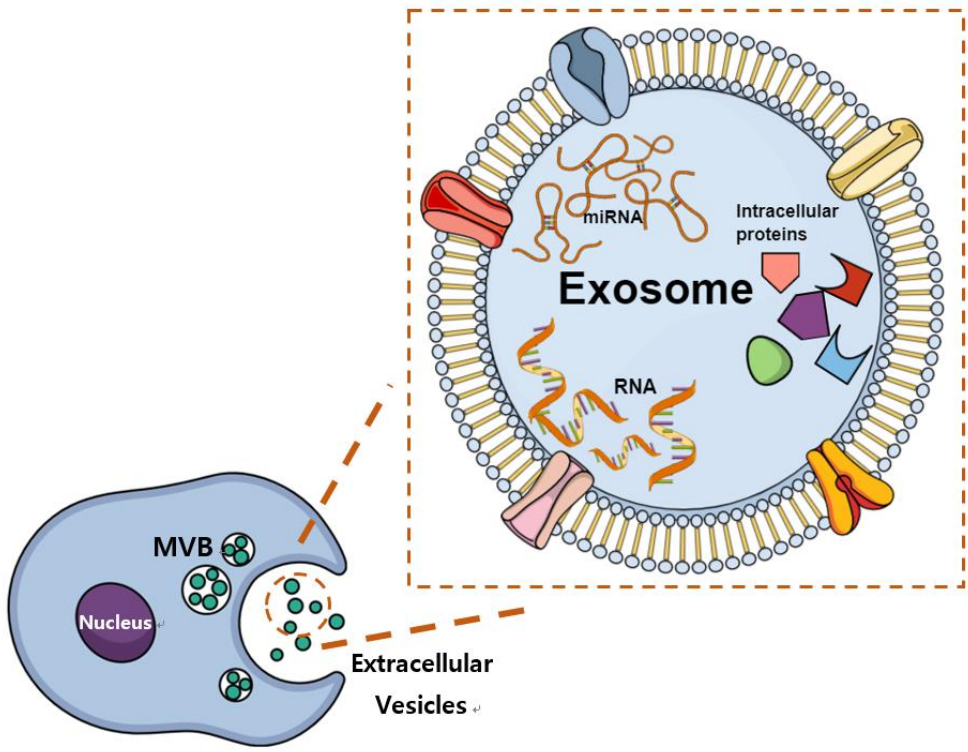

Figure 1. Extracellular vesicle (EV) and exosome biogenesis and secretion.

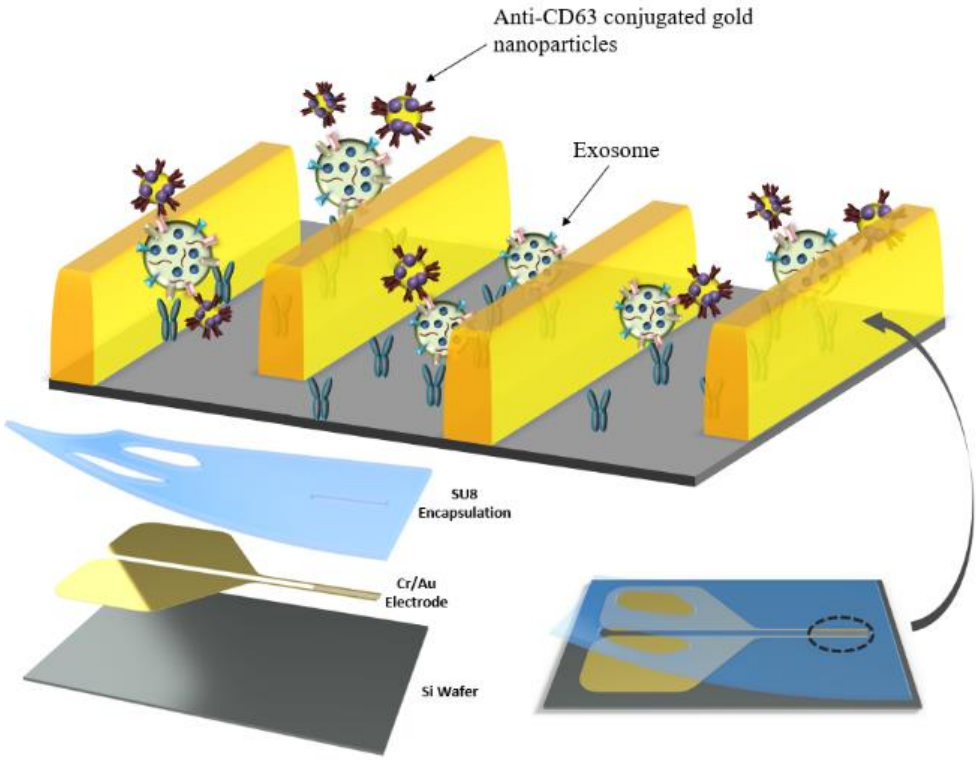

Figure 2. The overall schematic illustration of the interdigitated electrode (IDE) impedance-based biosensor with sensor fabrication layer.

Chapter 2. Materials and Methods

2.1. Materials

N-hydroxysuccinimide (NHS), (3-aminopropyl)triethoxysilane 99% (APTES), mercaptopoly(ethylene glycol) carboxylic acid (thiol-PEG-carboxylate, average Mn 2,100), sodium citrate dehydrate ($C_6H_5Na_3O_7 \cdot 2H_2O$), and tetrachloroauric (III) acid ($HAuCl_4 \cdot 3H_2O$), 11-mercaptoudecanoic acid 95% (11-MUA) were all purchased at Sigma-Aldrich (St. Louis, MO). *N*-Ethyl-*N* ' -(3-dimethylaminopropyl)carbodiimide hydrochloride (EDC) and Albumin Bovine Fraction V (BSA) were purchased from MP Biomedicals (Illkirch, Santa Ana, CA). Bis(sulfosuccinimidyl)suberate (BS^3) was purchased from Thermo Scientific (Rockford, IL). The anti-CD63 antibody and lyophilized exosomes from plasma of healthy donors were purchased at HansaBiomed Life Science (Tallin, Estonia). Phosphate buffer saline (PBS) was purchased from Welgene (Gyeongsangbuk-do, Korea). For all sample preparation was prepared through ultrapure water (Millipore Milli-Q grade).

2.2. Gold Nanoparticle Synthesis

Gold Nanoparticles synthesis was prepared based on the slightly modified standard citrate reduction process [30]. Briefly, an aqueous solution of 1 mM of $HAuCl_4$ was prepared and was heated with gentle stir until it was brought to boil. With a constant stirring and heating of the tetrachloraurate solution, 1% (v/v) of sodium citrate dehydrate was quickly added. After stirring for approximately for 10 min, the solution gradually changed its color to wine red from pale yellow. Then the solution was placed at room temperature to cool down after 15 min of reflux. Then it was stored at 4℃ for further use.

2.3. Conjugation of Anti-CD63 on Gold Nanoparticles

The schematic illustration of the preparation of anti-CD63 conjugated gold nanoparticle steps is shown in Figure 3. The gold nanoparticle surface was modified using 10mM of thiol-PEG-carboxylate. After preparing the 10 mM solution of thiol-PEG-carboxylate, it was then added to the 500 μL of the gold nanoparticle solution. It was incubated for 8 h at 4℃ to activate the reaction.

Afterward, thiol-PEG-carboxylate modified gold nanoparticles were washed and centrifuged twice at 8000g for 40 min at 4℃ (Gyrozen, Seoul, Korea) to remove excess thiol-PEG-carboxylate that were not activated. Following the removal of excess thiol-PEG-carboxylate, 100 mM of EDC and NHS were added to the PEG-carboxylate modified gold nanoparticle solution at a 1:1 ratio and were left to activate the reaction for 2 h at room temperature. Then again, the removal of excess EDC and NHS was proceeded by washing and centrifugation at 8000g for 40 min at 4℃. Then after EDC/NHS activated, gold nanoparticles were resuspended with PBS after centrifugation. Then 10 μg/mL of anti-CD63 was added and incubated overnight at 4℃. After incubation, 1% (w/v) BSA was added and incubated for 2 h for the blocking buffer to saturate excess protein-binding sites. The solution was then washed with PBS and stored at 4℃ for later use.

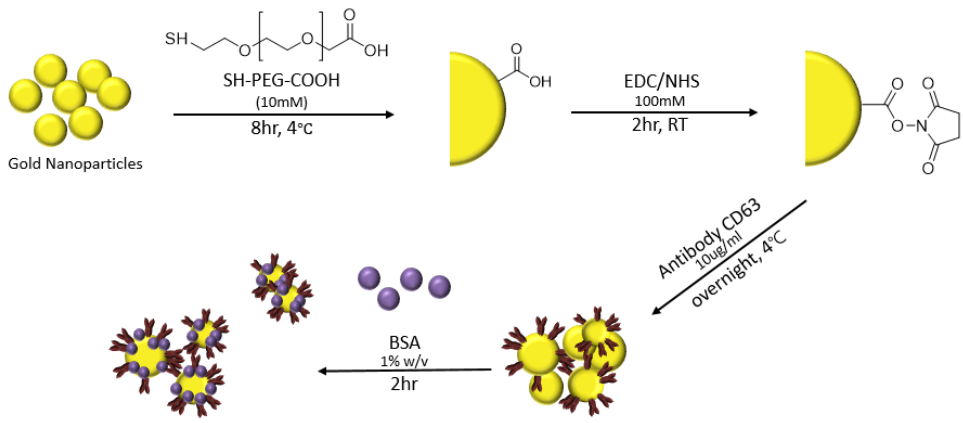

Figure 3. Schematic diagram of anti-CD63 conjugation onto the gold nanoparticles. Surface modification on the synthesized gold nanoparticles using thiol-PEG-carboxylate. The EDC/NHS activation and conjugation of anti-CD63 on the gold nanoparticles. BSA attachment after the conjugation of antibodies.

2.4. Sensor Fabrication

The Interdigitated electrode (IDE) sensor was fabricated using a standard photolithographic nano/microfabrication technique. Deposition and photolithographic patterning were done on bi-layers of Cr (10 nm)/Au (200nm) deposited on a cleanly prepared silicon wafer. After the fabrication of the gold interdigitated electrode sensor, 100 μm thick SU8-50 electrode encapsulation well was fabricated on the electrode. There are 23 pairs of interdigitated electrodes with 60 μm of spacing in between the electrodes. The self-assembly monolayer of 5 mM of 11-MUA was activated onto the interdigitated gold electrode surface for overnight to prevent the electrode surface contamination from large debris from non-specific binding during the steps of exosome immobilization shown in Figure 4a. Then, the electrodes were washed with ultrapure water.

2.5. Sensor Surface Modification

The hydroxyl group was activated in between the electrode using oxygen plasma (60 W, 80 sccm O_2) for 10 min. Afterward, the

electrodes were immersed in 5% (v/v) APTES at room temperature for an hour. It was then washed with ethanol and was placed on a hotplate at 100℃ for 30 min. Then freshly prepared 20 mM BS_3 (amine to amine crosslinker) was prepared in ethanol solution and activated onto the electrode for 30 min at room temperature. Following the BS_3 activation, 10 μg/mL of anti-CD63 was treated onto the activated electrodes and was incubated for 3 h at 4℃. After the incubation of anti-CD63, 5 μg/mL (2.5×10^{10} vesicles/mL) of the plasma-derived exosomes were drop-casted onto the electrode and were incubated in 4℃ for 30 min. Then the electrodes were washed with PBS to remove any unbound exosomes. Then anti-CD63 conjugated gold nanoparticles were added and incubated overnight at 4℃. The sensor was then washed with ultrapure water to remove any unbound anti-CD63 conjugated gold nanoparticles. Before the immobilization of the exosomes, impedance was measured after each step when the surface modification was made, shown in Figure 8.

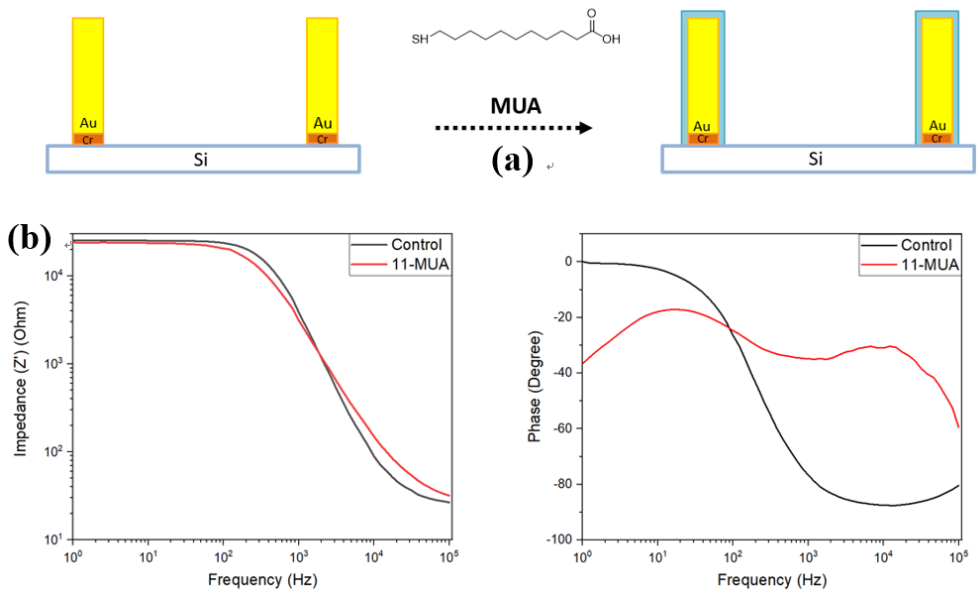

Figure 4. 11-mercaptoudecanoic acid (11-MUA) activation. (a) Schematic illustration of self-assembly monolayer of 5 mM of 11-MUA on the electrode surface. (b) Bode plot of impedance and phase of before and after 11-MUA treatment on the electrode.

Chapter 3. Results and Discussion

3.1. Characterization of Anti-CD63 Conjugated Gold Nanoparticles

The hydrodynamic diameter and zeta-potential of anti-CD63 conjugated gold nanoparticles were examined using a dynamic light scattering (Zetasizer Nano-ZS, Malvern Panalytical). The morphology and size determination were then characterized using a high-resolution transmission electron microscope (JEM3010, JEOL) with 300 kV of acceleration voltage. The sample preparation for HR-TEM was prepared on a thin carbon film-coated copper grid (300 mesh). UV-Visible spectroscopic measurement was acquired using a single beam spectrophotometer (Lambda 35 UV/VIS Spectrometer, PerkinElmer).

3.2. UV-Visible Spectrophotometry

The determination of the anti-CD63 conjugated gold nanoparticle solution took place through the optical technique of UV-visible

spectrophotometer, one of the important methods for characterizing colloidal gold nanoparticles. This optical method indicates the nanoparticle size distribution range through the width of the absorption spectra. It is known that the conventional citrate reduction method prepared gold nanoparticles to have the absorption peak that is observed at around 520 nm, which corresponds to the typical surface plasmon resonance (SPR)[31]. In this experiment, UV-vis spectra were measured between the 400 - 700 nm. Figure 5 shows the measured absorption peaks of three prepared samples, which are control colloidal gold nanoparticles, thiol-PEG-carboxylate modified gold nanoparticles, and anti-CD63 conjugated gold nanoparticles. In this study, the control colloidal gold nanoparticles' absorption peak was observed to be 524 nm. Then the absorption peak of anti-CD63 conjugated gold nanoparticles has shifted to 527 nm due to the presence of the thiol-PEG-carboxylate capsulation and the binding of the anti-CD63 onto the gold nanoparticle surface.

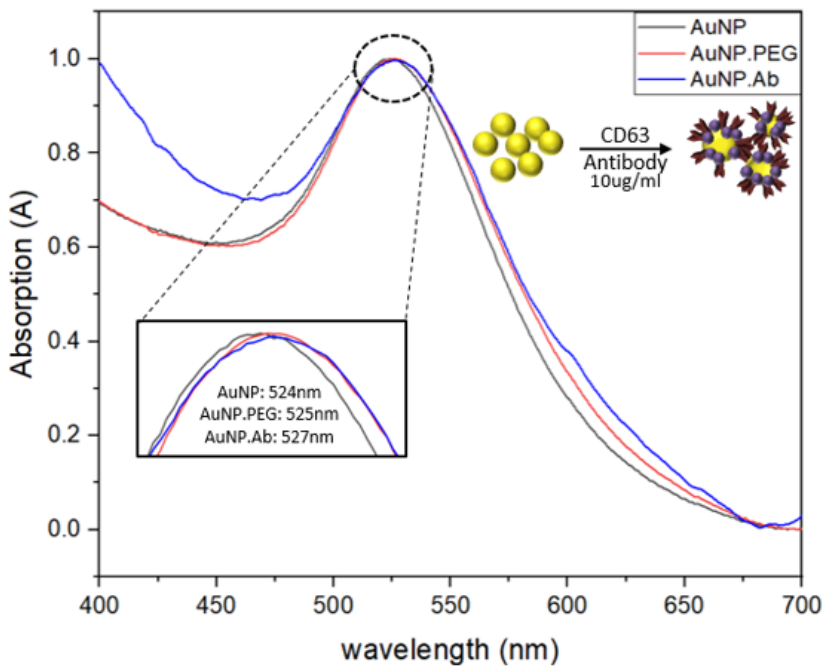

Figure 5. Characterization of anti-CD63 conjugated gold nanoparticles through UV-visible spectrophotometer. UV-visible spectra of control gold nanoparticle (AuNP), thiol-PEG-carboxylate modified gold nanoparticle (AuNP.PEG), and anti-CD63 conjugated gold nanoparticle (AuNP.Ab)

3.3. Zeta Size and Zeta-Potential

The mean hydrodynamic diameter and the zeta-potential of the control colloidal gold nanoparticles, thiol-PEG-carboxylate capped gold nanoparticles, and anti-CD63 conjugated gold nanoparticles were evaluated. The mean hydrodynamic diameter of the control colloidal gold nanoparticle was to be 23 nm, which shows a larger value compared to HR-TEM in Figure 6. This is because compared to the dried state prepared gold nanoparticles in HR-TEM, the solution state of gold nanoparticles is affected by the presence of the double layer in the calculation of the hydrodynamic radius in the DLS measurement [31]. The zeta-potential measurement of control colloidal gold nanoparticles and anti-CD63 conjugated gold nanoparticles were negatively charged, as shown in Table 1. The control colloidal gold nanoparticles had a zeta-potential of -35 mV, and then it increased to -22 mV for anti-CD63 conjugated gold nanoparticles. Knowing that the zeta-potential is affected by the thickness of the electrical double layer, that is, the electrical charge of the layer and the dielectric constant, it can be confirmed that the anti-CD63 has conjugated onto the gold nanoparticles [31].

	AuNP	AuNP.PEG	AuNP.Ab
Hydrodynamic Diameter	23.12 nm	28.68 nm	30.29 nm
Zeta-Potential	-35.8 mV	-34.7 mV	-22.9 mV

Table 1. Hydrodynamic diameter and zeta-potential measurement through dynamic light scattering.

3.4. High-Resolution Transmission Electron Microscopy, Transmission Electron Cryomicroscopy, and Fluorescence Microscopy

The use of high-resolution transmission electron microscopy took place to examine the size and the morphology of the synthesized gold nanoparticles and transmission electron cryomicroscopy was used to examine the exosomes. Figure 6a is an image of a control gold nanoparticle without any conjugation. Since the surface of the gold nanoparticles were not treated, the nanoparticles are not spread evenly. However, after the conjugation of anti-CD63 on the gold nanoparticles, it spread uniformly and orderly compared to the control colloidal gold nanoparticles with an average size of 20 nm shown in Figure 6b. Then, anti-CD63 conjugated gold nanoparticles were added to a solution with exosome shown in Figure 6d. As shown in Figure 6c, the anti-CD63 conjugated gold nanoparticles were well attached around the exosomes. The result of anti-CD63 conjugation onto the gold nanoparticles, the electrical double layer repulsive forces were formed around the conjugated gold nanoparticles preventing nanoparticles to agglomerate. Therefore, it can be confirmed that the anti-CD63 has been conjugated onto the gold

nanoparticle surface [31]. Then, characterization of fluorescence microscopy took place on the sensor surface as exosomes were immobilized. As shown in Figure 7b and c, it shows clear that the exosomes were successfully immobilized onto the modified sensor surface.

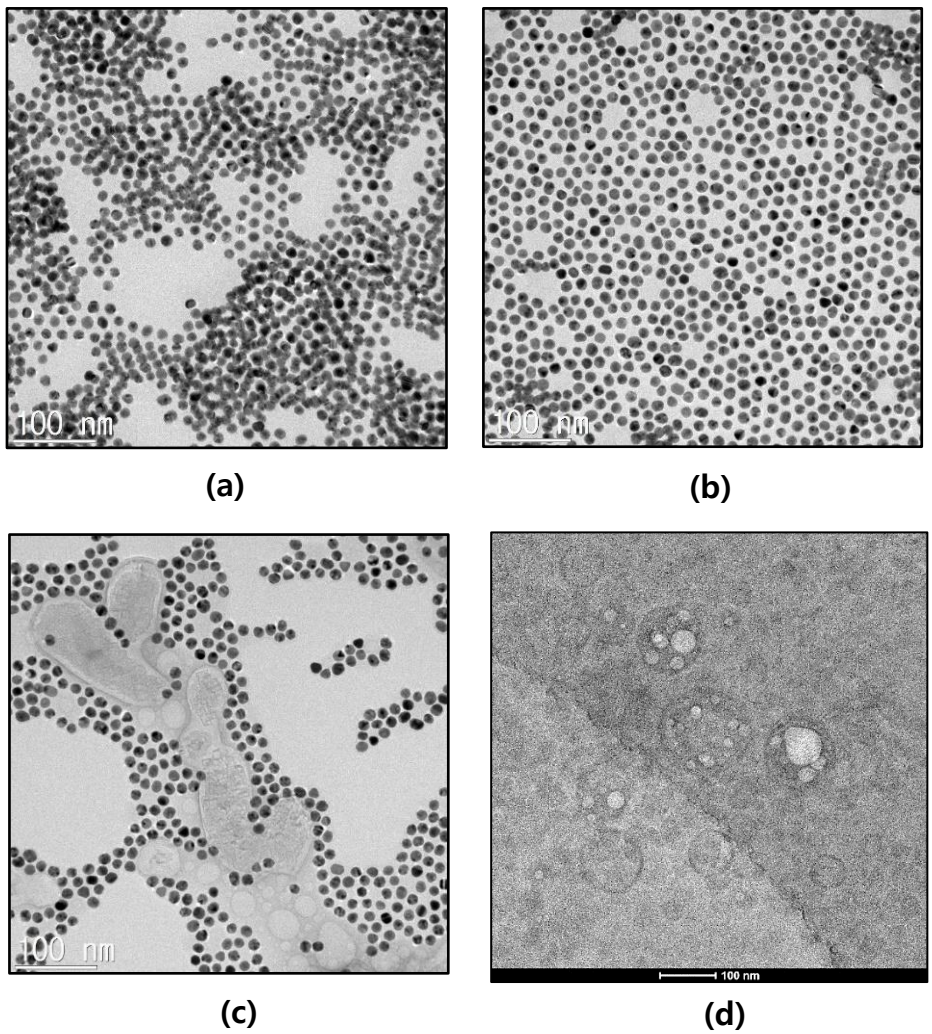

Figure 6. Image of high resolution-transmission electron microscopy (HR-TEM). (a) Citrate reduction prepared gold nanoparticle (control). (b) Anti-CD63 conjugated gold nanoparticles (c) Anti-CD63 conjugated gold nanoparticles bound to exosomes. (d) Transmission electron cryomicroscopy (Cryo-TEM) of exosome.

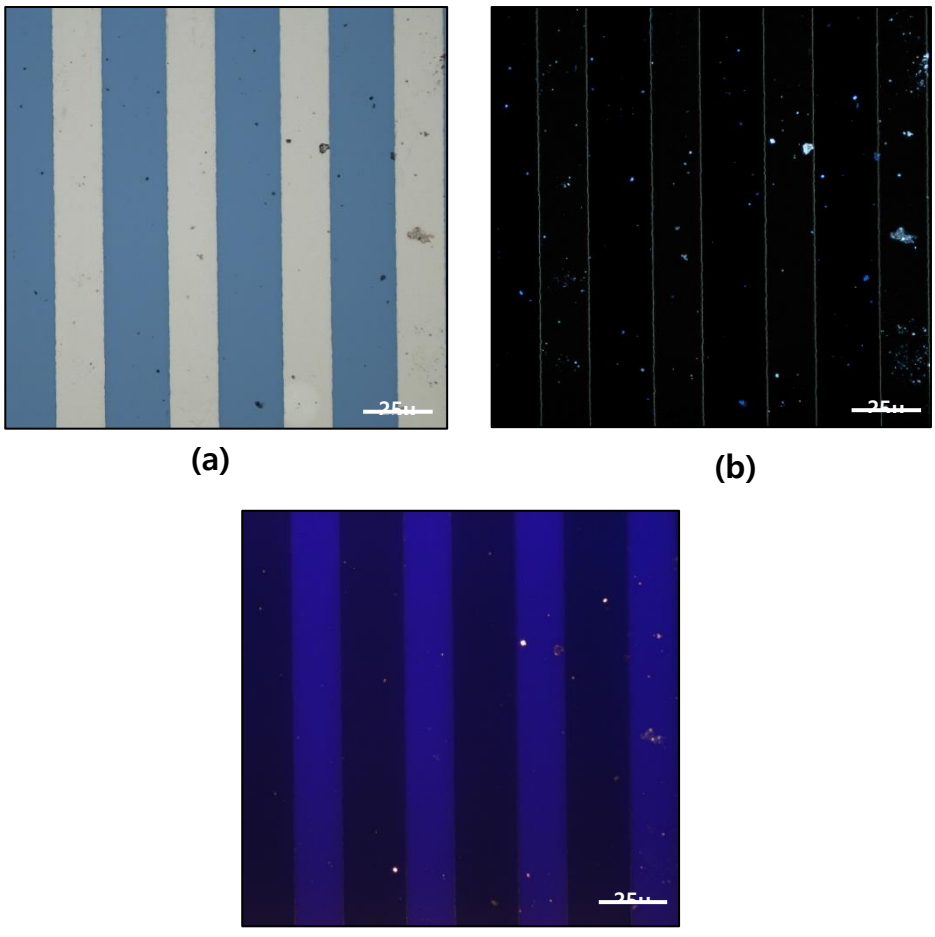

Figure 7. Image of fluorescence microscopy of immobilized exosomes. (a)Bright field image of sensor electrode with exosome. (b) Dark field image of sensor electrode with exosome (c) fluorescence image of sensor electrode with exosome (red).

3.5. Impedance Measurement

The impedance spectral measurements were carried out using Electrochemical Workstation (CHI614E, CH Instruments Inc.). The magnitude and phase of the impedance data were collected in the frequency range of 1 Hz to 100 kHz and by applying a voltage of 5 mV at room temperature. The baseline control measurement was performed using only PBS. Following control measurement, the impedance was measured after each step of immobilizing exosomes and binding of anti-CD63 conjugated gold nanoparticles onto the immobilized exosomes. To prevent unspecific binding and contamination of the electrode during the substrate surface modification steps, a monolayer of 11-MUA was self-assembled on the electrode, and impedance was measured, which is shown in Figure 4b. The magnitude of the impedance shows little to no change, yet the impedance phase component has shifted downward. This indicates an ideal result showing that the 11-MUA does not affect much change in the impedance magnitude and does not interfere with the impedance during the immobilization of the exosomes and binding of the anti-CD63 conjugated gold nanoparticles. The phase component of the impedance shifted downwards due to the capacitive

layer effect on the 11-MUA treated electrode [29]. After self-assembling a monolayer of 11-MUA, the substrate surface was modified to immobilize anti-CD63, and impedance was measured after each step of the substrate modification as shown in Figure 8a. The magnitude of the impedance has induced slightly. The phase has shifted further to the lower frequency due to its capacitive effect as chemical molecules are added onto each step.

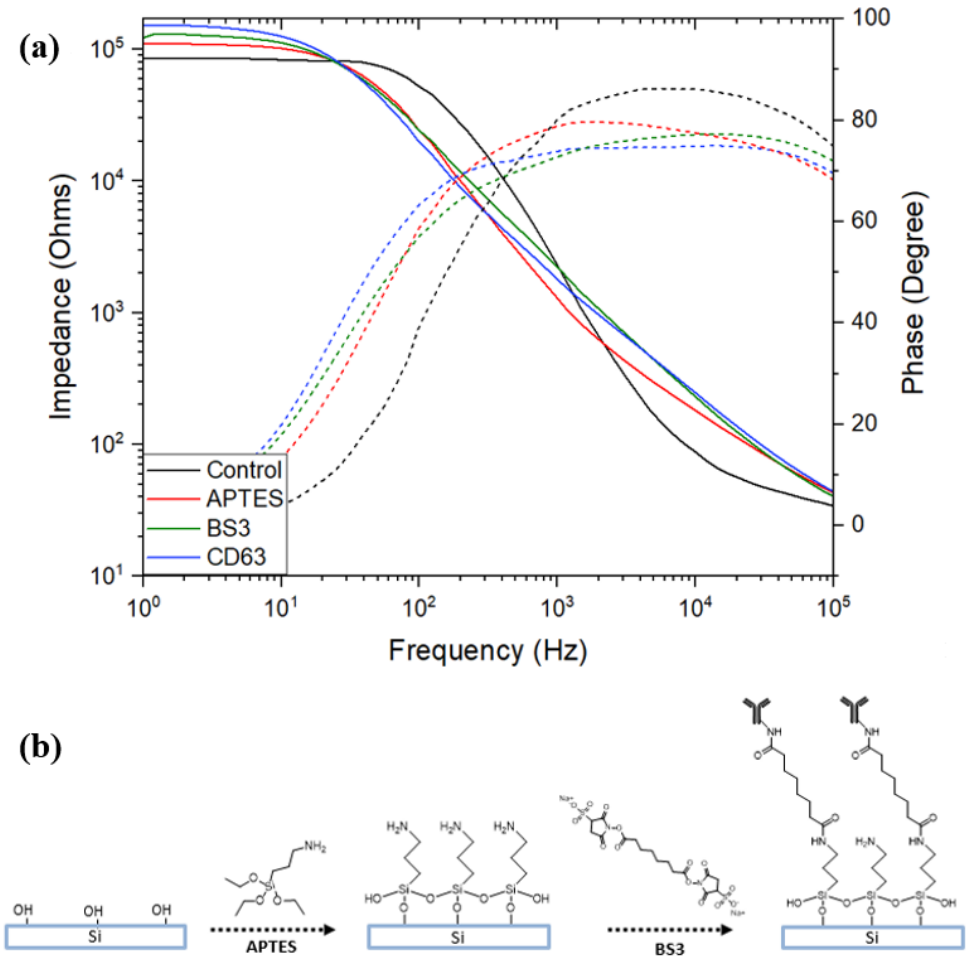

Figure 8. Sensor surface modification scheme and impedance measurement. (a) Bode plot of impedance and phase magnitude of surface modification steps of immobilizing anti-CD63. (b) Schematic illustration of immobilizing anti-CD63 on the substrate.

3.6. Equivalent Circuit Model and Analysis for Impedance Components

EIS's is one of the techniques that applies alternating current (AC) signal, a small amplitude voltage. Then the AC voltage signal scans a wide range of frequencies [25, 26]. The sensor is non-faradaic electrochemical impedance spectroscopy. It does not require the use of redox couples and a reference electrode. The mechanism of the non-faradaic EIS sensor of the absence and presence of the exosomes and anti-CD63 conjugated gold nanoparticles effect in the impedance is illustrated through the equivalent circuit model in Figure 9 [29, 32]. Before the immobilization of the exosomes, the equivalent circuit model contains only the double-layer capacitance of the electrodes (C_{dl}) in a series with the resistance of the base solution of PBS (R_{sol}). The electrodes are capsulated with a thin layer of charges as PBS is placed on the electrodes for control measurement, which makes a double layer capacitance on the electrode (C_{dl}) shown in Figure 9 [33]. Then, the addition of an impedance (Z_g) is added to the series of the equivalent circuit when the exosomes and anti-CD63 conjugated gold nanoparticles are added which the impedance (Z_g) contains the parallel of the exosomes and anti-CD63 conjugated gold nanoparticle resistance (R_g) and capacitance (C_g).

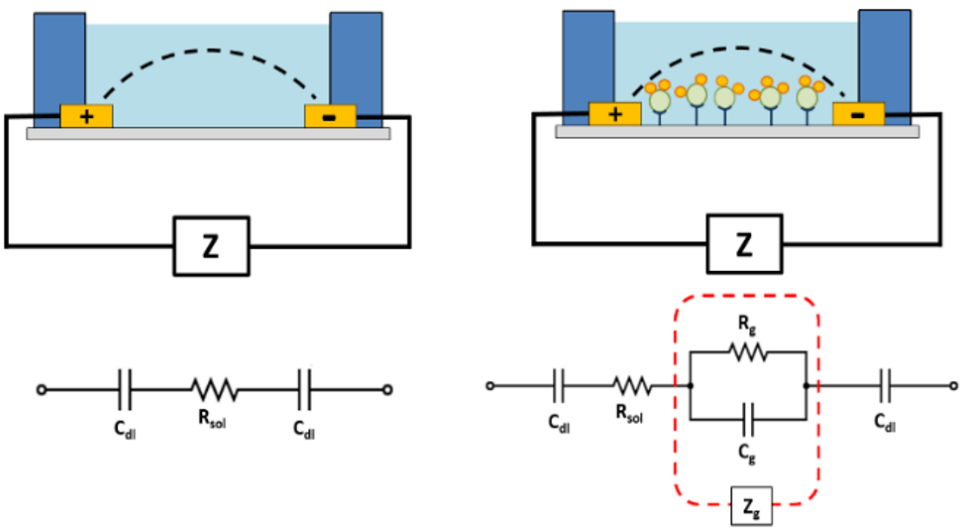

Figure 9. Equivalent Circuit Model. Illustration of the principles of the equivalent circuit of the electrochemical impedance spectroscopy before and after the immobilization of the exosomes and anti-CD63 conjugated gold nanoparticles.

3.7. Impedance Measurement of Exosomes and anti-CD63 Conjugated Gold Nanoparticles

The sensitivity of the impedance biosensor is affected as the surface of the sensor is modified with biomolecules, such as exosomes. When the exosomes were immobilized, the impedance change can be seen in the frequency range of 1 Hz to 10 kHz detecting 2.5 x 10^{10} vesicles/mL. The bode plot of before and after the immobilized exosomes and anti-CD63 conjugated gold nanoparticles are plotted, as shown in Figure 10. Before the capturing of the exosomes, the control impedance was measured to be 1.06 k Ω at 100 Hz. Then the impedance increased to 16.14 kΩ when the exosomes were immobilized in between the electrodes. To increase the sensitivity of the captured exosomes, the anti-CD63 conjugated gold nanoparticles were bound onto the exosomes, and the impedance has increased to 19.33 kΩ showing 19.76 % increase as the anti-CD63 conjugated gold nanoparticles were added. The SEM image of before and after the immobilization of the captured exosome and bound anti-CD63 conjugated gold nanoparticles are shown in Figure 11. The results show that the impedance has induced after the exosomes were immobilized, and anti-CD63 conjugated gold

nanoparticles were bound onto the exosomes. The change in the value of the impedance has induced due to the additional double layer capacitance (C_g) and the resistance (R_g) that are formed from the exosomes and anti-CD63 conjugated gold nanoparticles.

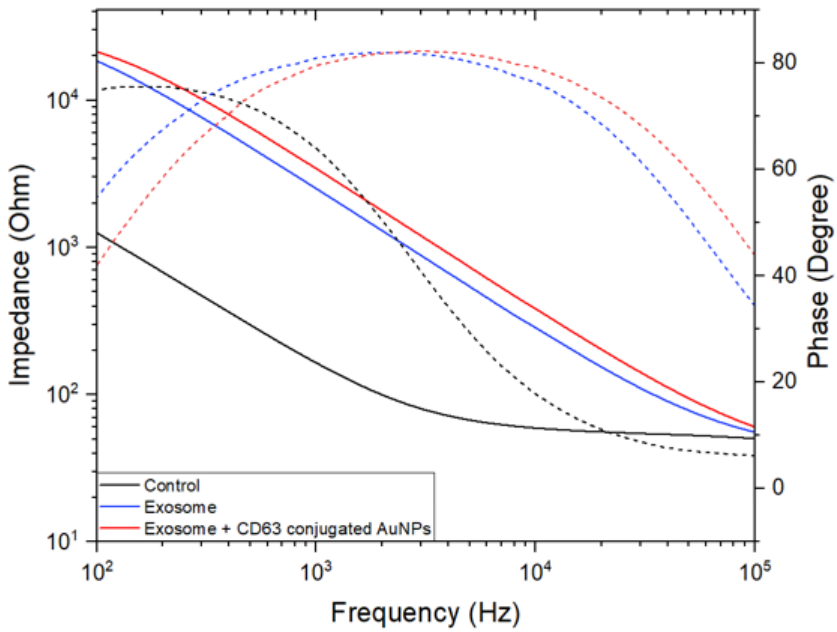

Figure 10. Impedance measurement of exosomes and anti-CD63 conjugated gold nanoparticles.

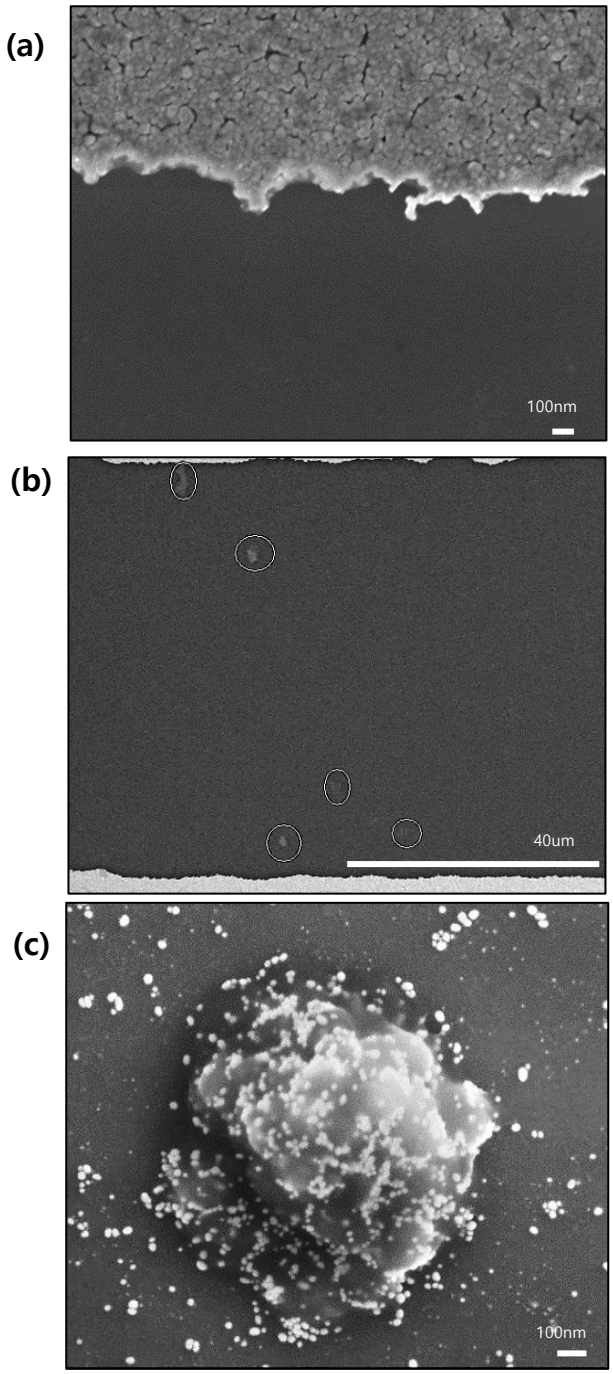

Figure 11. Field-emission scanning electron microscope (FE-SEM) image. (a) Electrode without exosome. (b, c) Electrode with exosome and bound anti-CD63 conjugated gold nanoparticles.

Chapter 4. Conclusion

In this study, an impedance-based biosensor with the application of interdigitated electrode has been fabricated. The surface of the biosensor was modified to capture human plasma-derived exosomes. When human plasma-derived exosomes were loaded onto the sensor, it has successfully captured and was able to detect through impedance measurement. To further induce the change in impedance, an additional binding of surface modified gold nanoparticle was applied. The anti-CD63 was conjugated onto the gold nanoparticles to specifically bind to the captured exosomes. As the anti-CD63 conjugated gold nanoparticles were attached to exosomes, it showed that the impedance has increased. The application of the conjugated gold nanoparticle has induced the change in the impedance, which indicates the sensitivity enhancement. Therefore, the proposed biosensor shows a promising technique that is capable to further expand the detection of exosomes as a diagnostic tool in clinical application. In future studies, the detection of various types of exosomes derived from cancer and neurodegenerative diseases experiments should be performed.

References

1. Lee, J., et al., *Enhanced paper-based ELISA for simultaneous EVs/exosome isolation and detection using streptavidin agarose-based immobilization.* Analyst, 2020. **145**(1): p. 157-164.
2. Maia, J., et al., *Exosome-Based Cell-Cell Communication in the Tumor Microenvironment.* Frontiers in cell and developmental biology, 2018. **6**: p. 18-18.
3. Zhang, W., et al., *Extracellular vesicles in diagnosis and therapy of kidney diseases.* American journal of physiology. Renal physiology, 2016. **311**(5): p. F844-F851.
4. Zhang, Y., et al., *Exosomes: biogenesis, biologic function and clinical potential.* Cell & bioscience, 2019. **9**: p. 19-19.
5. Ko, J., E. Carpenter, and D. Issadore, *Detection and isolation of circulating exosomes and microvesicles for cancer monitoring and diagnostics using micro-/nano-based devices.* The Analyst, 2016. **141**(2): p. 450-460.
6. Li, X., et al., *Challenges and opportunities in exosome research-Perspectives from biology, engineering, and cancer therapy.* APL bioengineering, 2019. **3**(1): p. 011503-011503.
7. Wu, M., et al., *Isolation of exosomes from whole blood by*

integrating acoustics and microfluidics. Proceedings of the National Academy of Sciences, 2017. **114**(40): p. 10584.

8. Ayala-Mar, S., et al., *Recent advances and challenges in the recovery and purification of cellular exosomes.* ELECTROPHORESIS, 2019. **40**(23-24): p. 3036-3049.

9. Im, H., et al., *Label-free detection and molecular profiling of exosomes with a nano-plasmonic sensor.* Nature Biotechnology, 2014. **32**(5): p. 490-495.

10. Reátegui, E., et al., *Engineered nanointerfaces for microfluidic isolation and molecular profiling of tumor-specific extracellular vesicles.* Nature Communications, 2018. **9**(1): p. 175.

11. Wang, S., et al., *Aptasensor with Expanded Nucleotide Using DNA Nanotetrahedra for Electrochemical Detection of Cancerous Exosomes.* ACS Nano, 2017. **11**(4): p. 3943-3949.

12. Su, J., *Label-Free Single Exosome Detection Using Frequency-Locked Microtoroid Optical Resonators.* ACS Photonics, 2015. **2**(9): p. 1241-1245.

13. Jeong, S., et al., *Integrated Magneto-Electrochemical Sensor for Exosome Analysis.* ACS Nano, 2016. **10**(2): p. 1802-1809.

14. Lee, J.-S. and C.A. Mirkin, *Chip-Based Scanometric Detection of Mercuric Ion Using DNA-Functionalized Gold*

Nanoparticles. Analytical Chemistry, 2008. **80**(17): p. 6805-6808.

15. Lee, J.-S., et al., *A DNA-Gold Nanoparticle-Based Colorimetric Competition Assay for the Detection of Cysteine.* Nano Letters, 2008. **8**(2): p. 529-533.

16. Mehta, B., Z. Li, and M. Zaghloul. *Optical biosensor using graphene nano ribbons*. in *2011 International Semiconductor Device Research Symposium (ISDRS)*. 2011.

17. Rodriguez, M.C., A.-N. Kawde, and J. Wang, *Aptamer biosensor for label-free impedance spectroscopy detection of proteins based on recognition-induced switching of the surface charge.* Chemical Communications, 2005(34): p. 4267-4269.

18. Chen, X., et al., *Electrical nanogap devices for biosensing.* Materials Today, 2010. **13**(11): p. 28-41.

19. Su, M., S. Li, and V.P. Dravid, *Microcantilever resonance-based DNA detection with nanoparticle probes.* Applied Physics Letters, 2003. **82**(20): p. 3562-3564.

20. Moulin, A.M., S.J. O'Shea, and M.E. Welland, *Microcantilever-based biosensors.* Ultramicroscopy, 2000. **82**(1): p. 23-31.

21. Arlett, J.L., E.B. Myers, and M.L. Roukes, *Comparative advantages of mechanical biosensors.* Nature nanotechnology,

2011. 6(4): p. 203-215.

22. Faria, R.A.D.d., et al., *Faradaic and non-faradaic electrochemical impedance spectroscopy as transduction techniques for sensing applications.* Internationla Journal of Biosensors & Bioelectronics, 2019. 5(1): p. 3.

23. Kazemi, S.H., M. Shanehsaz, and M. Ghaemmaghami, *Non-Faradaic electrochemical impedance spectroscopy as a reliable and facile method: Determination of the potassium ion concentration using a guanine rich aptasensor.* Materials science & engineering. C, Materials for biological applications, 2015. 52: p. 151-154.

24. Kostal, E., et al., *Impedimetric Characterization of Interdigitated Electrode Arrays for Biosensor Applications.* Proceedings, 2018. 2(13).

25. Wang, Y., Z. Ye, and Y. Ying, *New trends in impedimetric biosensors for the detection of foodborne pathogenic bacteria.* Sensors (Basel, Switzerland), 2012. 12(3): p. 3449-3471.

26. Prodromidis, M.I., *Impedimetric immunosensors—A review.* Electrochimica Acta, 2010. 55(14): p. 4227-4233.

27. Yusof, Y., et al., *Electrical characteristics of biomodified electrodes using nonfaradaic electrochemical impedance spectroscopy.* World Academy of Science, Engineering and

Technology, 2011. **73**.

28. Singh, K.V., et al., *3D nanogap interdigitated electrode array biosensors.* Analytical and bioanalytical chemistry, 2010. **397**(4): p. 1493-1502.

29. MacKay, S., et al., *Using Impedance Measurements to Characterize Surface Modified with Gold Nanoparticles.* Sensors (Basel, Switzerland), 2017. **17**(9): p. 2141.

30. Storhoff, J.J., et al., *One-Pot Colorimetric Differentiation of Polynucleotides with Single Base Imperfections Using Gold Nanoparticle Probes.* Journal of the American Chemical Society, 1998. **120**(9): p. 1959-1964.

31. Khashayar, P., et al., *Fabrication and Verification of Conjugated AuNP-Antibody Nanoprobe for Sensitivity Improvement in Electrochemical Biosensors.* Scientific Reports, 2017. **7**(1): p. 16070.

32. Mamouni, J. and L. Yang, *Interdigitated microelectrode-based microchip for electrical impedance spectroscopic study of oral cancer cells.* Biomedical Microdevices, 2011. **13**(6): p. 1075-1088.

33. Ghosh Dastider, S., et al., *Efficient and Rapid Detection of Salmonella Using Microfluidic Impedance Based Sensing.* Journal of Sensors, 2015. **2015**: p. 293461.

국문초록

표면 개질 된 금나노입자를 활용한 임피던스 기반 세포외소포 검출 바이오센서

정 한 나
나노융합전공
융합과학부
서울대학교 융합과학기술대학원

세포외소포는 유전자 물질 및 단백질과 같은 생물학적 물질을 함유하며, 세포 간에 정보 및 전달을 하는 중요한 역할을 가지고 있다. 이러한 세포외소포가 가지고 있는 특성으로 인하여 다양한 질병을 검출하기 위한 진단 도구로 사용할 수 있어 많은 관심과 연구가 진행되고 있다. 그러나, 나노 크기의 작은 세포외소포를 검출하고 분석할 수 있는 기술에 있어 어려움이 있는데, 현재 세포외소포를 검출 및 분석하기 위한 기술은 다소 복잡한 실험 절차가 있는 것 뿐만이 아니라 검사하고 측정하며 결과를 얻기까지의 시간이 길다는 한계점이 있다. 보다 빠른 분석을 위해, 본 연구에서는 임피던스 측정을 통해 세포외소포를 검출 및 분석을 하는 깍지형(interdigitated) 전극을 활용한 임피던스 기반

바이오센서가 개발되었다. 제작한 임피던스 기반 바이오센서의 감도를 향상하기 위해 anti-CD63 항체를 복합한 금 나노입자를 세포외소포에 결합하였다. 이 연구의 결과를 보았을 때, 세포외소포를 검출하기 전에는 1.055kΩ의 임피던스 값이 나왔는데, 세포외소포를 더하여 검출하였을 때 임피던스 값이 16.14kΩ으로 측정되어 증가한 것을 볼 수 있었다. 더 나아가 항체 anti-CD63를 복합한 금 나노입자를 검출한 세포외소포에 결합하였을 때에는 임피던스 값이 19.33kΩ으로 증가하여 세포외소포 만 검출하였을 때와 비교하면 19.76%의 임피던스 증가를 확인할 수 있었다. 본 연구에서 제안된 임피던스 기반 바이오센서 플랫폼은 세포외소포 검출에 대한 연구 기술 확장이 가능하며, 임상응용에서 진단도구로 사용될 수 있다.

주요어 : 세포외소포, 엑소좀, 임피던스 기반 센서, 바이오센서, 금나노입자

학 번 : 2018-27795